

UNIVERSITY OF SOUTHERN CALIFORNIA
DEPARTMENT OF CIVIL ENGINEERING

CORRELATIONS OF THE FREQUENCY DEPENDENT DURATION
OF STRONG GROUND MOTION WITH THE MODIFIED MERCALLI INTENSITY
AND THE DEPTH OF SEDIMENTS AT THE RECORDING SITE

by

B.D. Westermo and M.D. Trifunac

Report No. CE 79-01

A Report on Research Conducted Under a Contract From
the Nuclear Regulatory Commission

Los Angeles, California

February, 1979

ABSTRACT

The frequency dependent duration of strong ground motion and two related functionals have been correlated with the Modified Mercalli Intensity and the depth of sediments at the recording site. This work represents a refined extension of our previous study of the site geology effects upon the duration by classifying the local geology as either hard rock, soft deposits, or intermediate (Trifunac and Westermo, 1976b).

INTRODUCTION

Characteristics of strong ground motion such as the duration, $\int_0^T \{a^2, v^2, d^2\} dt$, and the average time rates of growth of these integrals (Trifunac and Westermo, 1976a,b) are dependent on the geology of the recording site. Correlations of these quantities with the recording site classification have shown that the duration of strong shaking can be as much as 12 seconds longer for a soft, alluvial site compared to a hard rock site, and values of $\int_0^T \{a^2, v^2, d^2\} dt$ and the average rate of growth of these functionals in time can vary by about an order of magnitude (Trifunac and Westermo, 1976a,b). In our previous work (Trifunac and Westermo, 1976a,b) the site characteristics were described by either $s=0$, 1 or 2 where $s=0$ represents sediments, $s=2$ stands for basement rock sites, and $s=1$ is for intermediate sites. This type of a site categorization did bring out the effects of the recording site geology, but could outline only the rough trends.

To refine the description of the effects of geology on duration of strong motion we propose to characterize the site geology by the depth of sediments to bedrock at the site. This depth, of course, does not completely describe the site effects but it appears to represent one of the more significant features of the site geometry for purposes of wave propagation studies. This depth is often available from geological surveys.

In previous studies (Trifunac and Westermo, 1976a,b) we have examined regressions of the duration, $\int_0^T \{a^2, v^2, d^2\} dt$, and the

average rate of growth of these integrals in terms of the Modified Mercalli Intensity, the frequency of motion, and the site classification. We re-examine these regressions in this report by replacing the site classification with the depth of sediments and we quantify the fit of the data to the model equations in terms of approximate distribution functions.

DEFINITIONS AND A DESCRIPTION OF THE DATA

The integrals of the form $\int_0^T \{a^2, v^2, d^2\} dt$, where $a(t)$, $v(t)$, and $d(t)$ represent the acceleration, velocity and displacement, and T is the record length, are related to various characteristics of strong ground motion and in particular to the different measures of instrumental intensity (Arias, 1970; Housner, 1952), the seismic wave energy, and the expected maximum values of the peaks of $a(t)$, $v(t)$, and $d(t)$ (Trifunac and Brady, 1975; Trifunac and Westermo, 1976a,b). These integrals generally increase rapidly with the onset of the strong motion and then gradually tend to their maxima, $\int_0^T \{a^2, v^2, d^2\} dt$. Using these functions of the strong earthquake motion, we define the duration as the sum of the time intervals which make the largest contributions to 90% of the final value, $\int_0^T \{a^2, v^2, d^2\} dt$ (Trifunac and Westermo, 1976a,b). Figure 1 graphically summarizes this definition of duration.

The average rate of growth of integrals $\int_0^t \{a^2, v^2, d^2\} d\tau$ is defined as

$$\text{Rate} \begin{Bmatrix} a \\ v \\ d \end{Bmatrix} = \int_0^T \begin{Bmatrix} a^2 \\ v^2 \\ d^2 \end{Bmatrix} dt / \text{Duration} \begin{Bmatrix} a \\ v \\ d \end{Bmatrix} . \quad (1)$$

This rate represents the average of the slopes of $\int_0^t \{a^2, v^2, d^2\} d\tau$ for the time intervals of strong motion.

The data used in this study was taken from 186 strong ground motion records which were the result of 57 earthquakes in the western United States. These complete records were successively low-pass

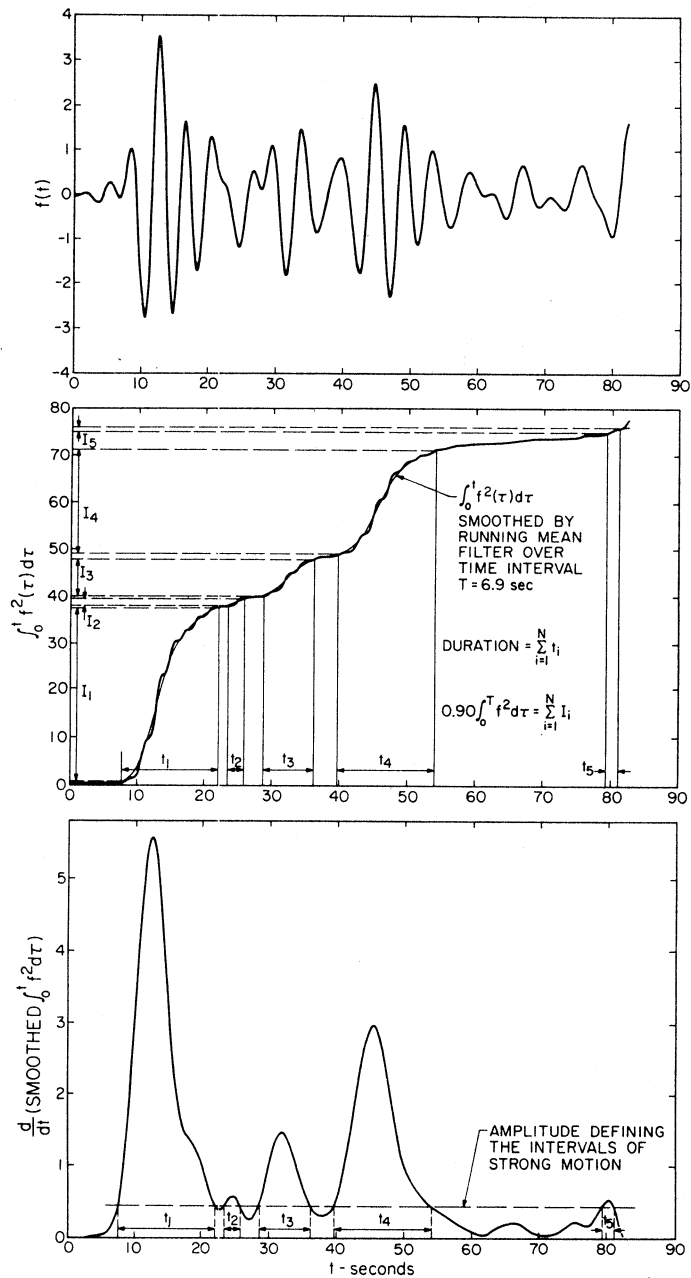


Figure 1

Top: Record for displacement from Kern County earthquake after application of the band-pass filter centered at 0.22 cps.

Middle: Comparison of $\int_0^t f^2(\tau) d\tau$ computed for $f(t)$ in the top figure with its smoothed form.

Bottom: The derivative of the smoothed function, $\int_0^t f^2(\tau) d\tau$, showing the intervals of strong motion as defined in this paper (after Trifunac and Westermo, 1976a).

filtered to decompose the routinely processed (Trifunac and Lee, 1973) strong motion records into six frequency bands with the center frequencies at $f_c = 0.22, 0.5, 1.1, 2.75, 7.0$ and 18.0 Hz. Other details on this data can be found in a report by Trifunac and Westermo (1976a).

The depths used in this analysis represent the geologic thickness of the sediments on top of sound, basement rock. Those depths are meant to portray the "characteristic length" to the "most prominent" impedance jump beneath the recording site. The data consists of sites with depths between zero km (hard rock sites) and 6.4 km with 82% of the data having a depth of 4 km or less.

CORRELATIONS OF THE DURATION OF STRONG GROUND MOTION
WITH THE MODIFIED MERCALLI INTENSITY (MMI) AND THE
DEPTH OF SEDIMENTS AT THE RECORDING SITE

We consider the simple linear regression equation of the form

$$\text{Duration} \begin{Bmatrix} a \\ v \\ d \end{Bmatrix} = a(\omega_c) + b(\omega_c)I_{MM} + c(\omega_c)h \quad , \quad (2)$$

where I_{MM} is the intensity level on the MMI scale, h represents the depth of sediments in km, and $\omega_c = 2\pi f_c$. For reasons already described in our earlier analysis (Westermo and Trifunac, 1978) only the term $c(\omega_c)h$ is used to represent the contribution to the duration from the site geology effects. Second order and higher terms do not lead to coefficients significantly different from zero. The remaining terms, $a(\omega_c) + b(\omega_c)I_{MM}$, model the trend of duration with respect to I_{MM} .

The coefficients $a(\omega_c)$, $b(\omega_c)$, and $c(\omega_c)$ are determined by the least squares fitting of equation (2) to the data. As in the previous analyses (Trifunac and Westermo, 1976a,b) the data for the high frequency displacement and low frequency acceleration bands were omitted from the fitting procedure because of their low signal to noise ratio.

The frequency bands used in low-pass filtering the original data are sufficiently narrow so that it is possible to employ the approximation

$$\begin{aligned} \text{Duration}\{v(t)\} &\simeq \text{Duration}\{a(t)\} \quad , \\ \text{Duration}\{d(t)\} &\simeq \text{Duration}\{a(t)\} \quad , \end{aligned} \quad (3)$$

and thus combine all three duration data sets into one regression analysis. The vertical and horizontal components of motion were analyzed separately.

The scatter of the computed duration data about the model, equation (2), is characterized by calculating the residuals

$$\varepsilon = \text{Duration} \begin{pmatrix} a \\ v \\ d \end{pmatrix} - \{a(\omega_c) + b(\omega_c)I_{MM} + c(\omega_c)h\} \quad (4)$$

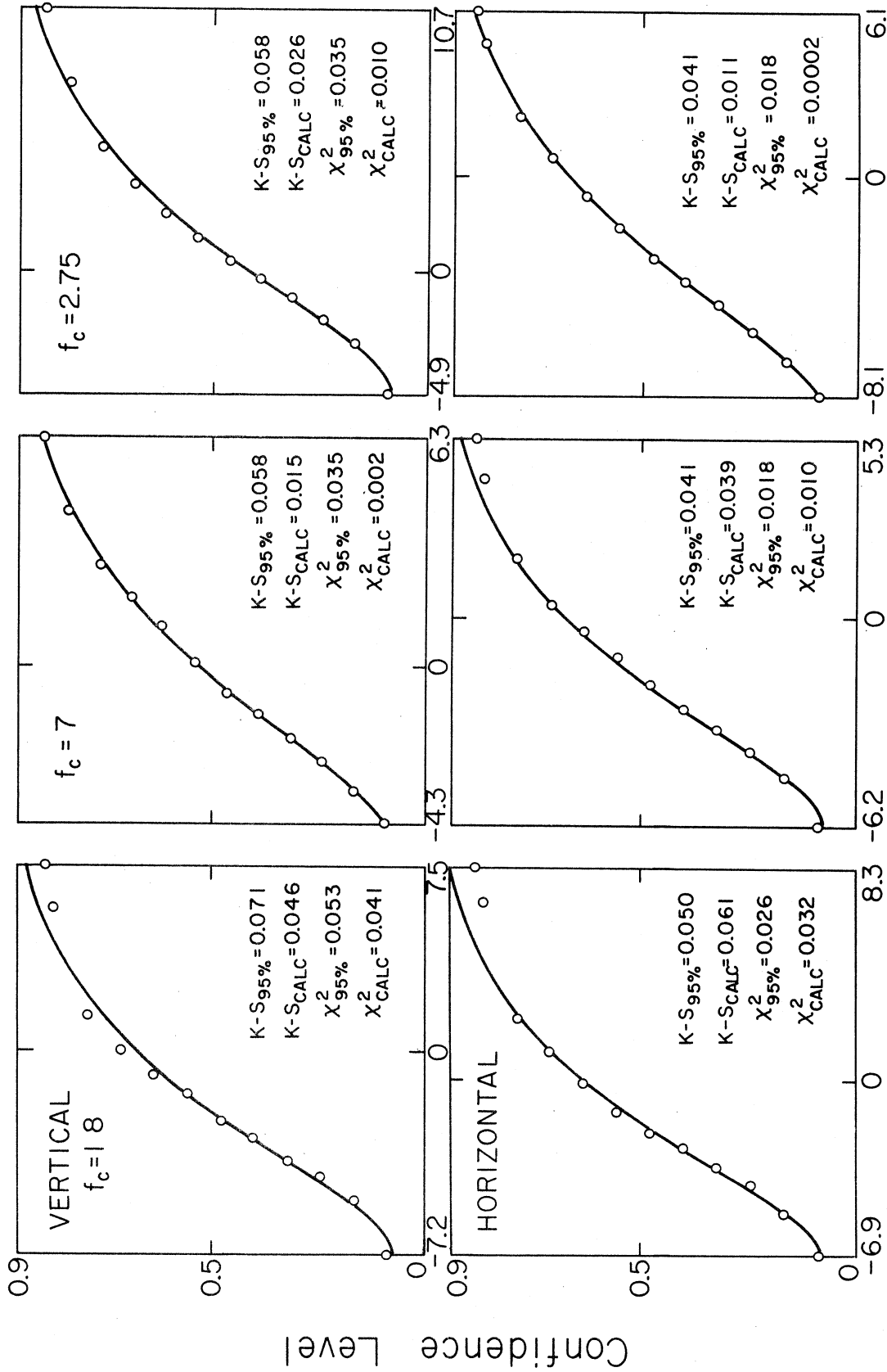
Figures 2a and 2b present these residuals (open circles) and their analytical approximations (continuous lines) plotted versus "confidence level," the probability that they will not be exceeded. For the regression analysis of duration in terms of magnitude, epicentral distance, and depth of sediments (Westermo and Trifunac, 1978) a double exponential distribution of the form

$$p(\varepsilon) = 1 + \alpha_1 e^{\beta_1 \varepsilon} + \alpha_2 e^{\beta_2 \varepsilon} \quad (5)$$

were found to fit the distribution of residuals fairly well. The same distribution (equation (5)) has been chosen to represent the residuals in (4), and the coefficients α_1 , α_2 , β_1 and β_2 were calculated from the least square fitting of the distribution in equation (5) to the data on ε . These coefficients are shown in Figure 3a versus ω_c .

Table I lists the coefficients a , b , c , α_1 , α_2 , β_1 and β_2 for all six frequency bands and both components of motion. The variances of a , b and c , determined from the regression, are also listed in Table I. The coefficients $a(\omega_c)$, $b(\omega_c)$ and $c(\omega_c)$ and their 95% confidence intervals are shown plotted versus the center frequency, ω_c , in Figure 3b.

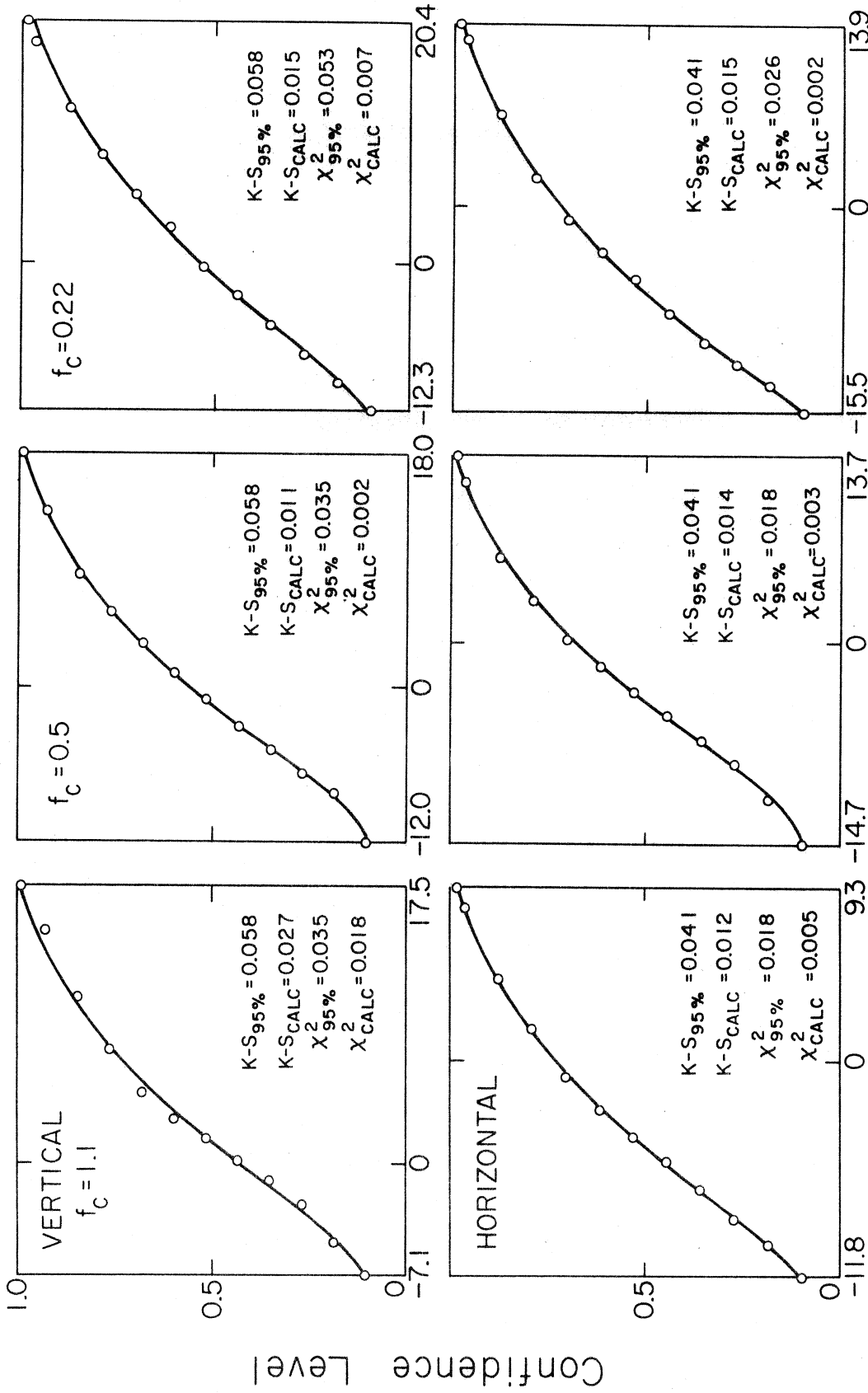
The trend of the intensity dependent term, $b(\omega_c)I_{MM}$, indicates that the duration decreases with increasing I_{MM} for all of the frequency bands. The duration decreases by roughly 5 seconds per I_{MM} at



$\epsilon(\omega_c)$

Figure 2a

The confidence level, p , versus the residual, ϵ , for the calculated residuals (circles) and for the fitted double exponential distribution (solid curve). The Chi-Squared and Kolmogorov-Smirnov criteria are listed for each distribution.



$\epsilon(\omega_c)$

Figure 2b

The confidence level, p , versus the residual, ϵ , for the calculated residuals (circles) and for the fitted double exponential distribution (solid curve). The Chi-Squared and Kolmogorov-Smirnov criteria are listed for each distribution.

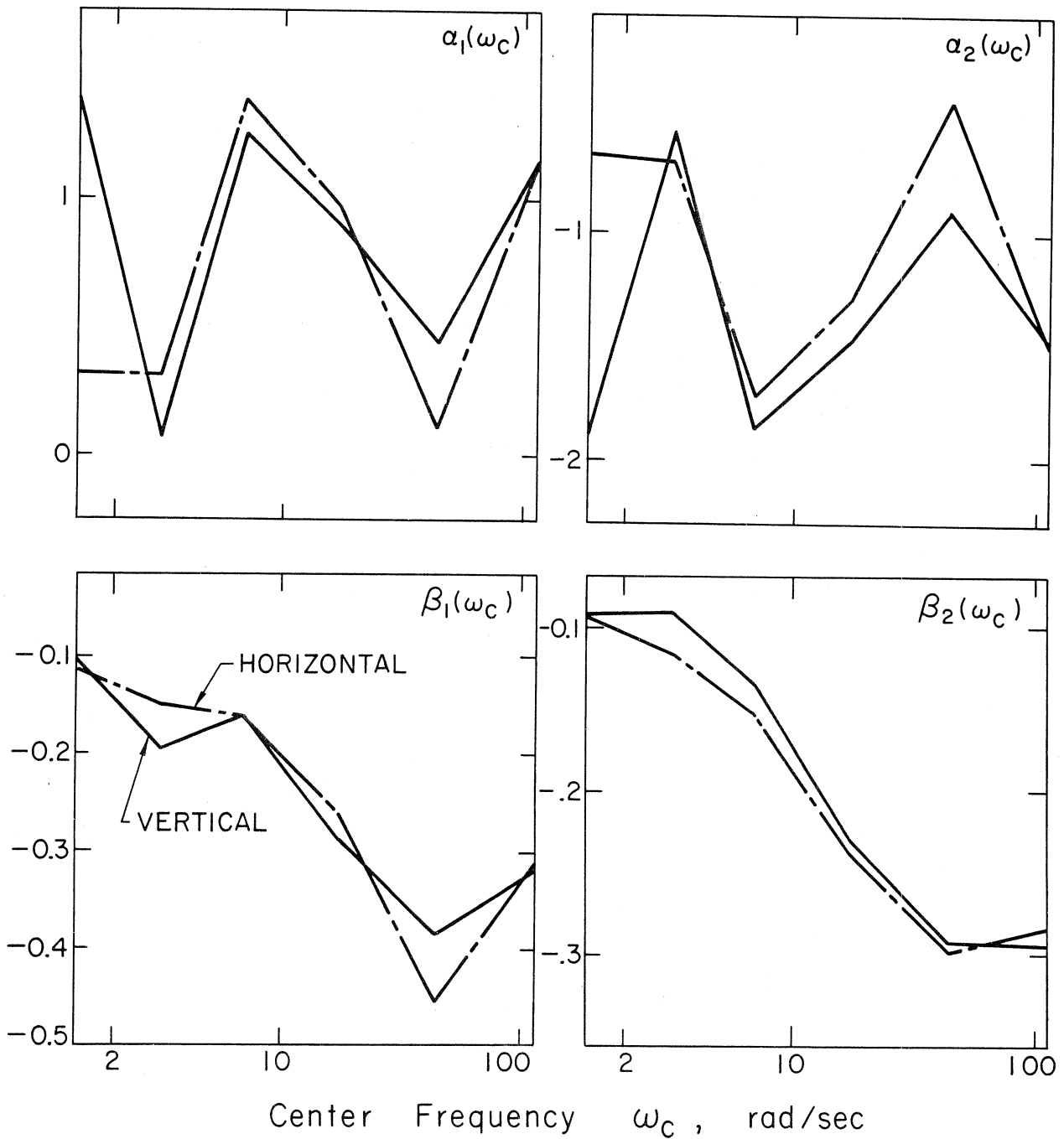


Figure 3a

The coefficients α_1 , α_2 , β_1 and β_2 in equation (5) for the vertical and horizontal components and plotted versus $\omega_c = 2\pi f_c$ (for $f_c = 0.22, 0.5, 1.1, 2.75, 7.0$ and 18.0 Hz).

TABLE I

Regression Coefficients in Duration $\begin{Bmatrix} a \\ v \\ d \end{Bmatrix} = a + bI_{MM} + ch$

VERTICAL COMPONENT

	$f_c = 18.0$	$f_c = 7.0$	$f_c = 2.75$	$f_c = 1.1$	$f_c = 0.5$	$f_c = 0.22$
a	2.458	1.762	2.261	3.313	4.576	5.531
Variance(a) (x0.1)	0.307	0.186	0.197	0.250	0.342	0.429
b	-2.295	-1.348	-1.968	-3.008	-3.946	-5.290
Variance(b)	0.480	0.290	0.308	0.391	0.535	0.665
c	1.211	0.908	1.579	1.734	1.679	1.422
Variance(c)	0.240	0.145	0.154	0.196	0.268	0.332
α_1	1.160	0.439	0.887	1.248	0.072	1.397
β_1 (x10)	-3.190	-3.852	-2.881	-1.601	-1.946	-1.027
α_2	-1.485	-0.906	-1.473	-1.863	-0.567	-1.914
β_2 (x10)	-2.954	-2.935	-2.304	-1.332	-0.892	-0.908
No. of Data	372	558	558	558	558	372

HORIZONTAL COMPONENTS

	$f_c = 18.0$	$f_c = 7.0$	$f_c = 2.75$	$f_c = 1.1$	$f_c = 0.5$	$f_c = 0.22$
a	2.719	2.027	2.563	3.644	4.281	5.362
Variance(a) (x0.1)	0.202	0.125	0.153	0.193	0.240	0.339
b	-2.755	-1.676	-2.326	-3.340	-3.458	-4.686
Variance (b)	0.316	0.196	0.239	0.301	0.375	0.526
c	1.095	0.882	1.770	2.112	2.080	1.230
Variance (c)	0.158	0.098	0.119	0.151	0.188	0.262
α_1	1.145	0.108	0.963	1.381	0.305	0.313
β_1 (x10)	-3.111	-4.539	-2.614	-1.631	-1.511	-1.147
α_2	-1.508	-0.429	-1.290	-1.723	-0.695	-0.664
β_2 (x10)	-2.841	-2.987	-2.386	-1.522	-1.142	-0.921
No. of Data	744	1116	1116	1116	1116	744

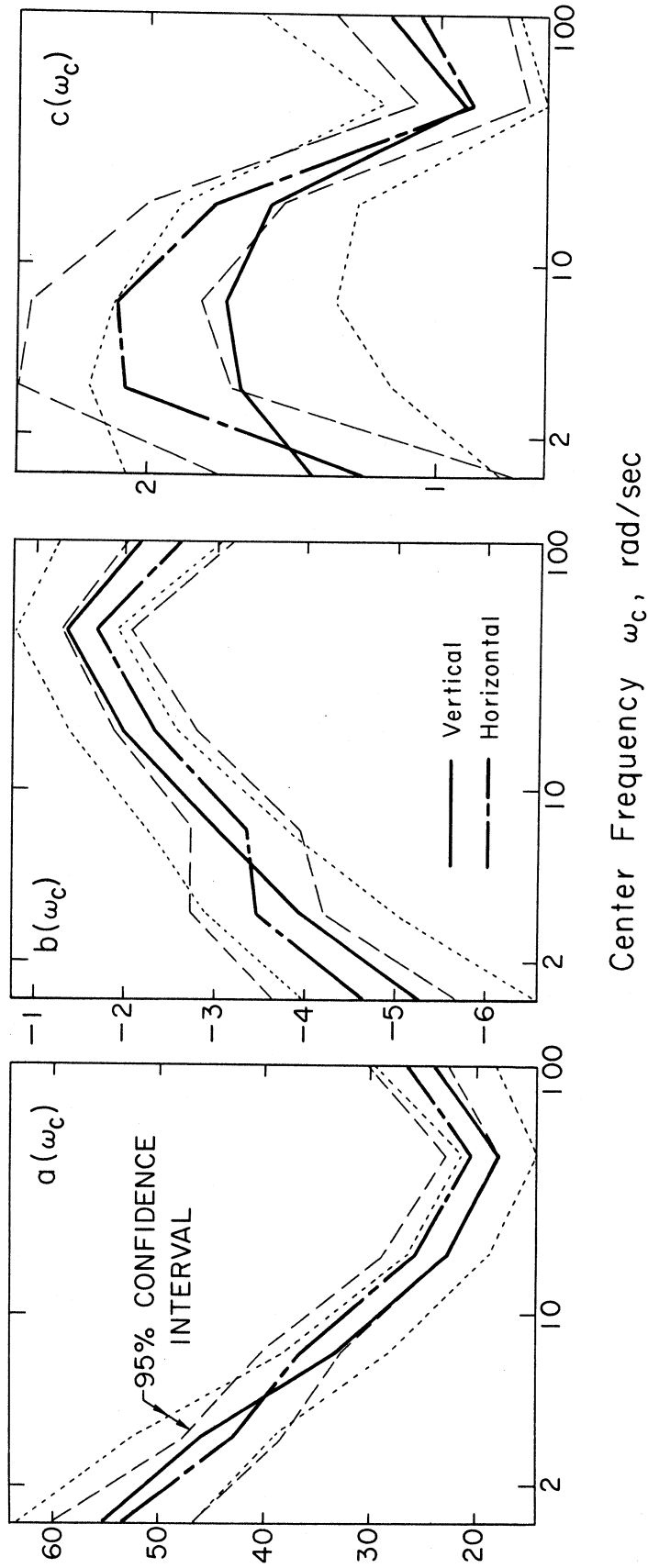


Figure 3b

The coefficients a , b , and c in equation (2) for the vertical and horizontal components and plotted versus $\omega_c = 2\pi f_c$ (for $f_c = 0.22, 0.5, 1.1, 2.75, 7.0$ and 18.0 Hz). The coefficients are bounded by their calculated 95% significance intervals.

$f_c = 0.22$ Hz and by less than about 2 seconds per I_{MM} at $f_c = 7.0$ Hz.

The curve for $c(\omega_c)$ in Figure 3b shows that the increase in the duration with depth of sediments is at a maximum for $f_c = 1.1$ Hz where the duration increases by over 2 secs/km for the horizontal motions and by roughly 1.7 secs/km for the vertical motions. The dependence of the model in equation (2) on depth is similar to that of the similar regression in terms of magnitude (Figure 3 in Westermo and Trifunac, 1978). The differences are that for the horizontal motions $c(\omega_c)$ is greater than for the vertical motions at $f_c = 0.5, 1.1$ and 2.75 Hz for the regression model in terms of I_{MM} , while the duration for vertical motions is longer than for the horizontal motions at the same frequencies for the magnitude dependent regression.

Other functional forms of the empirical scaling for the duration of strong motion in terms of the Modified Mercalli Intensity and depth of sediments were examined. In one of those, a quadratic dependence of the duration on depth of the form

$$\text{Duration} \begin{Bmatrix} a \\ v \\ d \end{Bmatrix} = a' + b'I_{MM} + c'h + d'h^2 \quad (6)$$

was examined. Since the effects of the sedimentary layer on the duration should be small for both small and large depths (relative to the wavelength of the problem), the quadratic depth dependent term was chosen to find whether such trends can be detected in the data. The coefficient c' was found to be significantly different from zero at the 95% confidence level for 6 of the 12 fits, while d' was significantly different from zero for only 2 of these fits. This resulted

most likely because the depth data does not contain large enough depths to fully cover the expected trends. The linear dependence of the duration on the depth of sediments was thus chosen as in equation (2) to model the duration of strong shaking for small to moderate depths.

The equation

$$\text{Duration} \begin{Bmatrix} a \\ v \\ d \end{Bmatrix} = a'' + b''I_{MM} + c''h + d''I_{MM}h \quad (7)$$

was also analyzed and fitted to the data. The mixed term, $d''I_{MM}h$, was used in equation (7) to examine the possible significance of coupling effects of I_{MM} and h on computed durations. The coefficient $d''(\omega_c)$ was not, however, significantly different from 0 at the 95% confidence level.

The coefficients listed in Table I were smoothed along the frequency axis by applying a $\frac{1}{4}, \frac{1}{2}, \frac{1}{4}$ weight filter to the six frequencies of each coefficient. The duration, as given by equation (2), was then calculated using these smoothed coefficients for several intensities and depths and is shown in Figure 4. Here it is seen that the duration is as much as 16 seconds longer for the low frequencies ($f_c = 0.22$ and 0.5 Hz) than for the high frequencies ($f_c = 18.0$ and 7.0 Hz). This variation is more pronounced for greater depths and lower Modified Mercalli Intensities. The curves in Figure 4 show a smaller variation in the relative increases in duration with the depth than was noted for the corresponding magnitude correlations (Westermo and Trifunac, 1978). This could be partly due to the regression of equation (2) interpreting the larger dispersion at high frequencies as a

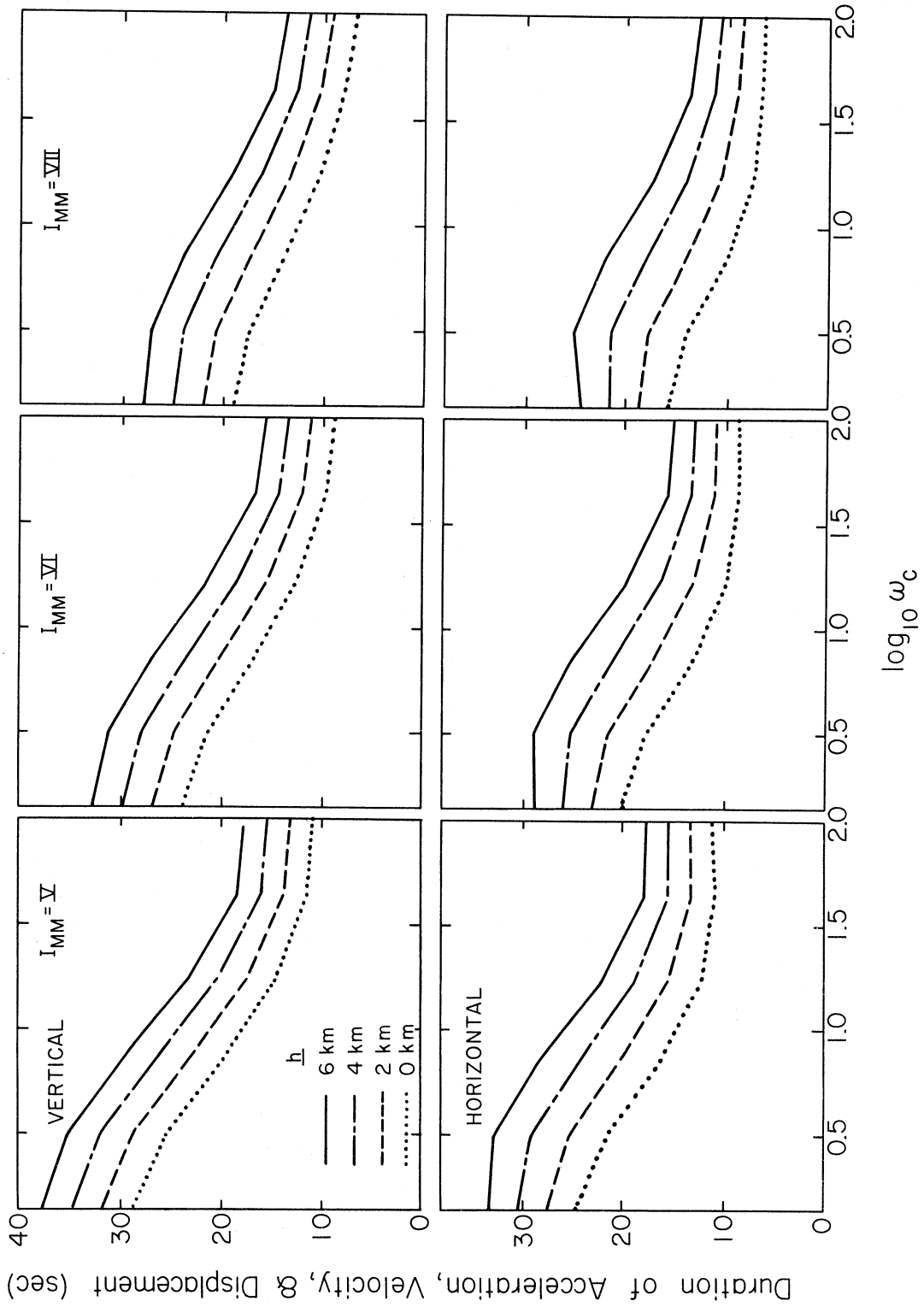


Figure 4
 The duration of strong ground motion as calculated from equation (2) (with $\epsilon = 0$) versus frequency for various intensities and depths.

depth dependent effect, since equation (2) has not explicit dependence of the duration on the epicentral distance. This can also results from the implicit dependence of the Modified Mercalli Intensity on both the recording site geology and the epicentral distance.

CORRELATIONS OF $\log_{10} \int_0^T a^2(t)dt$, $\log_{10} \int_0^T v^2(t)dt$, AND
 $\log_{10} \int_0^T d^2(t)dt$ WITH THE MODIFIED MERCALLI INTENSITY AND
 THE DEPTH OF SEDIMENTS AT THE RECORDING SITE

The correlation of the integrals $\int_0^T \{a^2, v^2, d^2\}dt$ with the Modified Mercalli Intensity and the depth of sediments are examined in this section in terms of the following empirical model

$$\log_{10} \int_0^T \left\{ \begin{array}{c} a^2 \\ v^2 \\ d^2 \end{array} \right\} dt = a + bI_{MM} + ch + dh^2 \quad (8)$$

The dependence of the integrals on h was assumed to be quadratic following our previous correlations of $\log_{10} \int_0^T \{a^2, v^2, d^2\}dt$ with the magnitude and depth of sediments (Westermo and Trifunac, 1978). As previously mentioned, the effects of the sedimentary layer on duration of strong shaking should be small for depths much less than the characteristic wavelength of strong shaking. For large depths, the anelastic attenuation attenuates the reflected waves. Hence, the contribution to the integrals from $ch + dh^2$ should approach zero for both great and small depths. A quadratic dependence was chosen to approximately represent this assumed trend whose functional form is as yet not known.

The acceleration, velocity and displacement data were combined into one regression analysis by assuming that the frequency bands are sufficiently narrow to be represented by their center frequencies, ω_c . Then we find

$$\log_{10} \int_0^T v^2 dt \approx \log_{10} \int_0^T a^2 dt - 2 \log_{10} \omega_c \quad (9a)$$

$$\log_{10} \int_0^T d^2 dt \approx \log_{10} \int_0^T a^2 dt - 4 \log_{10} \omega_c \quad (9b)$$

The velocity and displacement data were "converted" by the above equations and combined with the acceleration data to correlate equation (8) for $\log_{10} \int_0^T a^2 dt$ only. Changing $a(\omega_c)$ in equation (8) via equations (9) will yield the results for the integrals of velocity and displacement squared in equation (8).

A regression equation involving mixed dependence of the integrals on the depth of sediments and intensity of the form

$$\log_{10} \int_0^T a^2(t) dt = a' + b' I_{MM} + c' h + d' I_{MM} h \quad (10)$$

was also applied to the data. The coefficient $d'(\omega_c)$ was not different from zero at a 95% confidence level. Thus, such possible dependence on depth and Modified Mercalli Intensity parameters was neglected and equation (8) was chosen as the final regression model.

The coefficients a , b , c and d as calculated by the regression of equation (8) with the acceleration and acceleration corrected velocity and displacement data (using equations (9)) are listed in Table II. Plots of these coefficients versus center frequency are shown in Figure 5.

The residuals given by

$$\varepsilon = \log_{10} \int_0^T a^2(t) dt - \left\{ a + b I_{MM} + c h + d h^2 \right\} \quad (11)$$

are presented as a distribution, $p(\varepsilon)$, where p corresponds to the confidence that ε will not be exceeded. These distributions are shown in Figures 6a and 6b. As with the magnitude correlations (Westermo

TABLE II

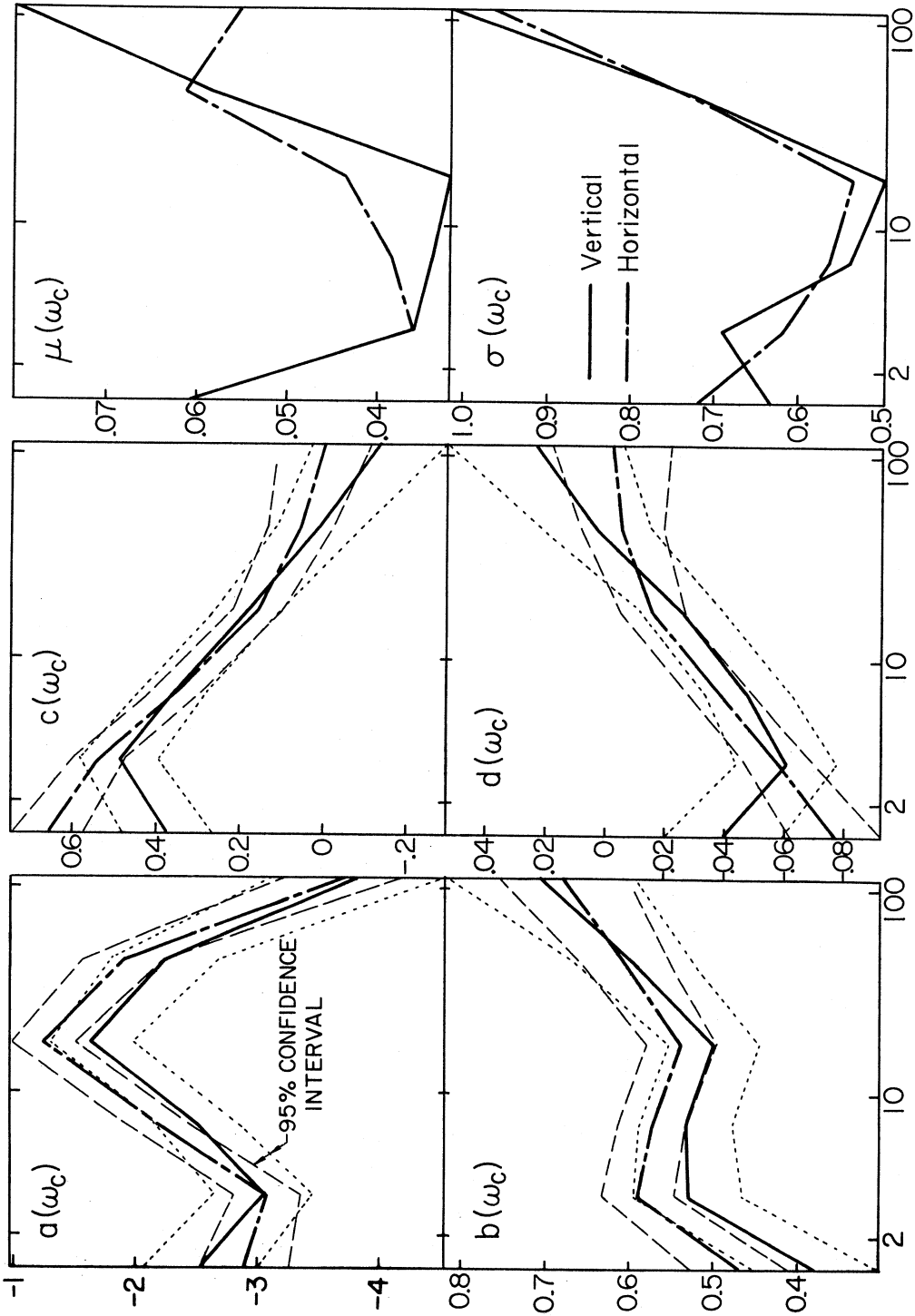
Regression Coefficients in $\log_{10} \int_0^T a^2(t) dt = a + bI_{MM} + ch + dh^2$

VERTICAL COMPONENT

	$f_c = 18.0$	$f_c = 7.0$	$f_c = 2.75$	$f_c = 1.1$	$f_c = 0.5$	$f_c = 0.22$
a	-2.841	-1.241	-0.640	-1.506	-2.049	-1.534
Variance(a)	0.359	0.227	0.172	0.177	0.205	0.240
b	7.062	5.955	4.986	5.323	5.290	3.773
Variance(b) (x10)	0.573	0.362	0.274	0.282	0.327	0.383
c	-1.355	0.093	1.778	3.535	4.867	3.721
Variance(c) (x10)	0.830	0.525	0.397	0.408	0.474	0.554
d	2.348	0.306	-2.577	-4.765	-6.045	-3.965
Variance(d) (x100)	1.491	0.943	0.713	0.734	0.852	0.996
μ (x100)	8.000	5.830	3.193	3.390	3.580	6.080
σ (x10)	10.158	7.257	4.957	5.370	6.918	6.323
h_{max}	2.885	-1.532	3.451	3.710	4.025	4.692
No. of Data	372	558	558	558	558	372

HORIZONTAL COMPONENT

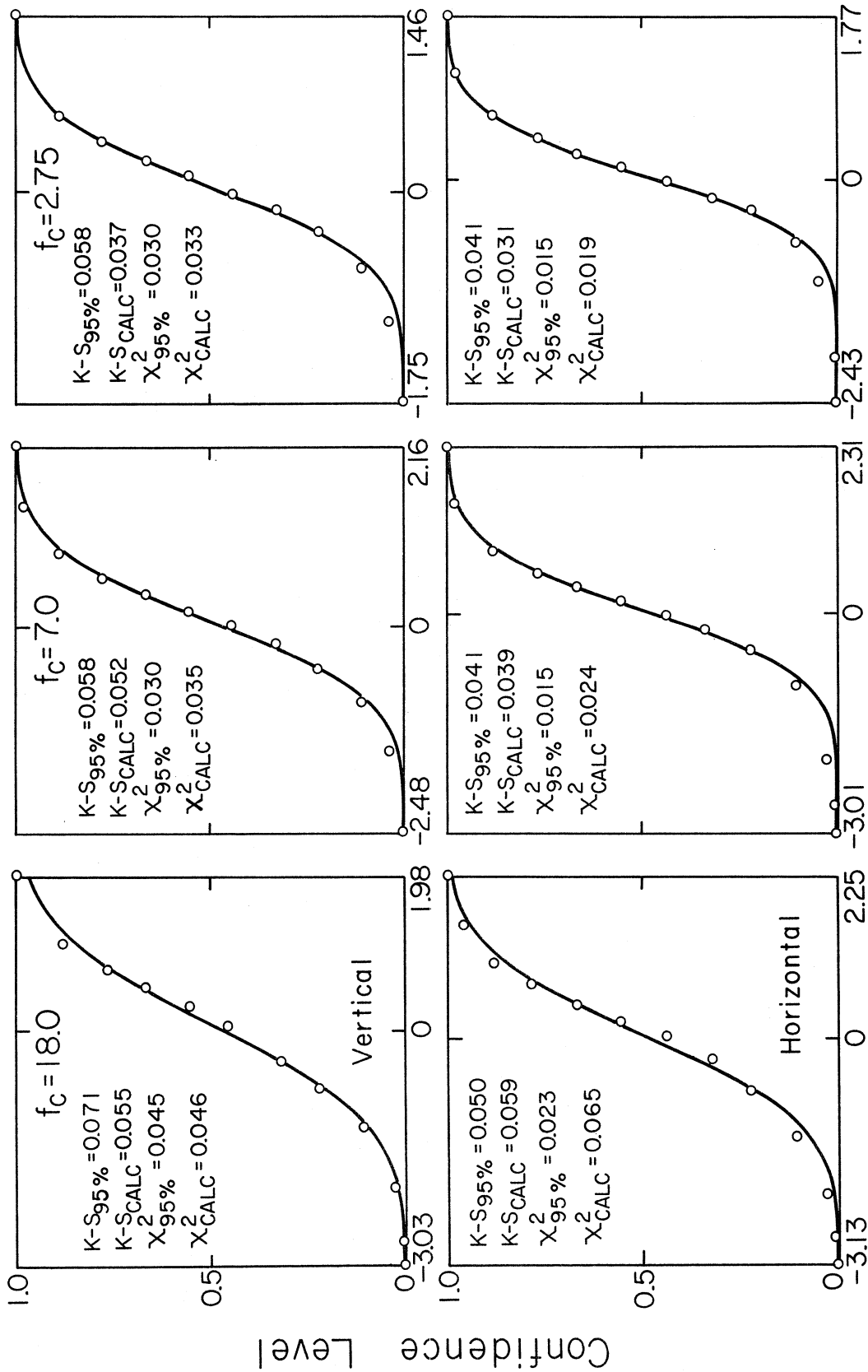
	$f_c = 18.0$	$f_c = 7.0$	$f_c = 2.75$	$f_c = 1.1$	$f_c = 0.5$	$f_c = 0.22$
a	-2.736	-0.905	-0.248	-1.183	-2.083	-1.891
Variance(a)	0.246	0.172	0.133	0.132	0.139	0.187
b	6.799	6.058	5.370	5.719	5.891	4.682
Variance(b) (x10)	0.392	0.274	0.212	0.211	0.222	0.299
c	-0.039	0.528	1.553	3.453	5.381	6.574
Variance(c) (x10)	0.569	0.398	0.308	0.306	0.322	0.433
d	-0.193	-0.522	-1.564	-3.865	-5.806	-7.708
Variance(d) (x100)	1.022	0.715	0.554	0.550	0.579	0.778
μ (x100)	5.500	6.132	4.359	3.840	3.600	6.070
σ (x10)	9.650	7.289	5.346	5.622	6.185	7.204
h_{max}	-1.016	5.053	4.964	4.466	4.633	4.265
No. of Data	744	1116	1116	1116	1116	744



Center Frequency ω_c , rad/sec

Figure 5

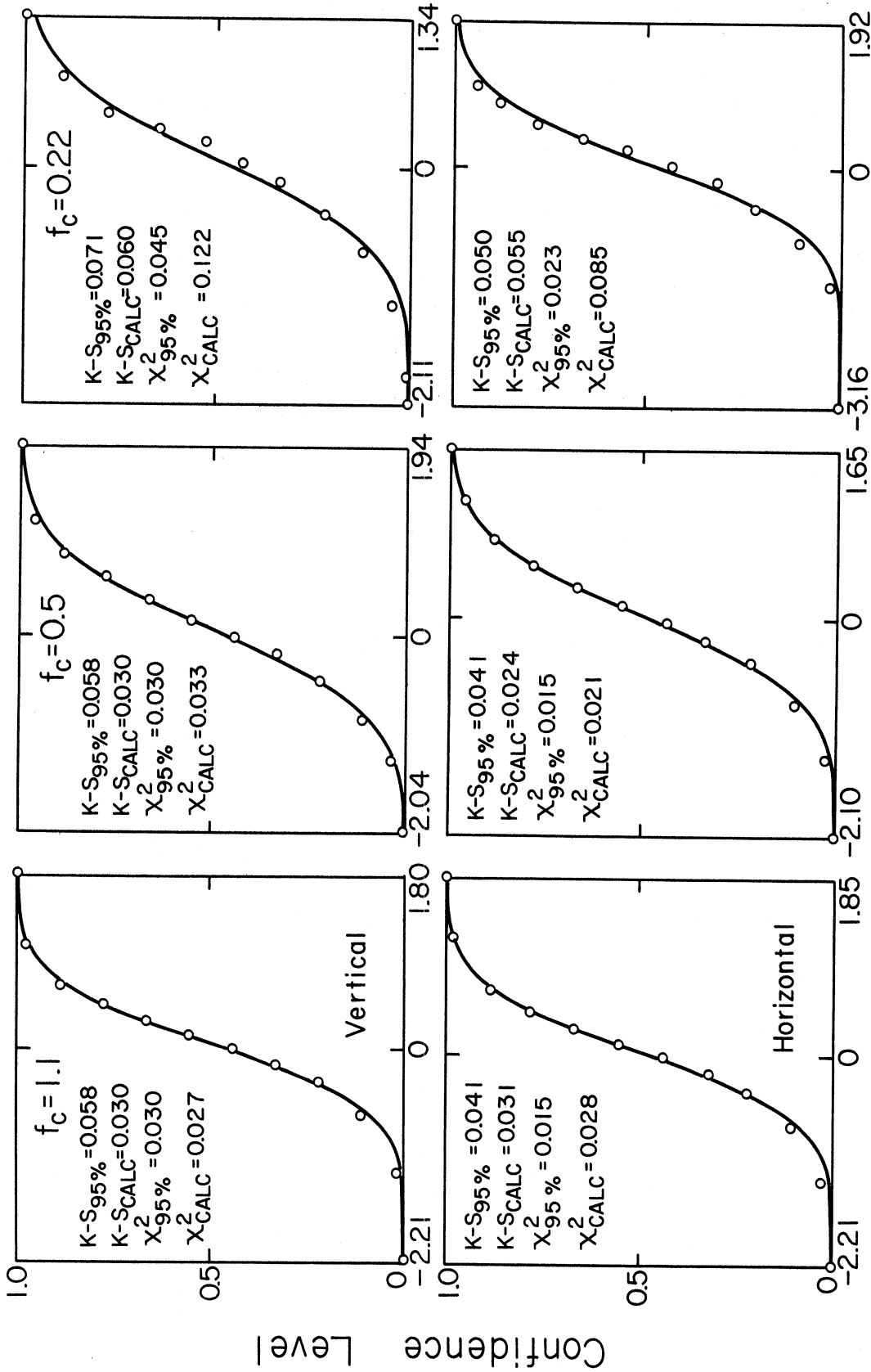
The coefficients a , b , c , d , μ , and σ in equations (8) and (12) for the horizontal and vertical accelerations and plotted versus $\omega_c = 2\pi f_c$ (for $f_c = 0.22, 0.5, 1.1, 2.75, 7.0$ and 18.0 Hz). The coefficients a , b , c and d are bounded by the 95% confidence interval.



$\epsilon(\omega_c)$

Figure 6a

The confidence level, p , versus the residual, ϵ , for the calculated residuals (circles) and for the fitted Gaussian distribution (solid curve). The Chi-Squared and Kolmogorov-Smirnov test results are listed for each distribution.



$\epsilon (\omega_c)$

Figure 6b

The confidence level, p , versus the residual, ϵ , for the calculated residuals (circles) and for the fitted Gaussian distribution (solid curve). The Chi-Squared and Kolmogorov-Smirnov test results are listed for each distribution.

and Trifunac, 1978), a normal distribution of the form

$$p(\epsilon) = \frac{1}{\sqrt{2\pi}} \int_{-\infty}^{\frac{\epsilon-\mu}{\sigma}} e^{-\frac{1}{2}x^2} dx \quad (12)$$

was fitted to the $p(\epsilon)$ data. As shown in Figures 6a and 6b all but two of the assumed distributions passed the Kolmogorov-Smirnov test at the 95% confidence level. Only one distribution passed the corresponding Chi-Squared test. Nevertheless, the Gaussian distributions were adopted as sufficiently representative as described by the mean, $\mu(\omega_c)$, and standard deviation, $\sigma(\omega_c)$ (equation (12)). The resulting μ and σ are listed in Table II and are shown plotted versus frequency in Figure 5.

From the plot of $b(\omega_c)$, it is seen that the integrals increase with the intensity for all frequencies by as much as 0.7 per I_{MM} (on the log scale) at $f_c = 18.0$ Hz and as little as 0.45 per I_{MM} for the low frequencies ($f_c = 0.22$ Hz). For the four lowest frequency bands ($f_c = 0.22, 0.5, 1.1$ and 2.75 Hz), the horizontal component shows a larger dependence on the intensity than does the vertical component.

Figure 7 presents the values of $c_s h + d_s h^2$ versus depth for the coefficients c and d smoothed along ω_c as previously mentioned for Figure 4. These functions have a similar behavior for the four lowest frequency bands, $f_c = 0.22, 0.5, 1.1$ and 2.75 Hz, with their maxima lying between 3 and 5 km. The coefficients $c(\omega_c)$ and $d(\omega_c)$ are not significantly different from zero for $f_c = 18.0$ and 7.0 Hz, and so

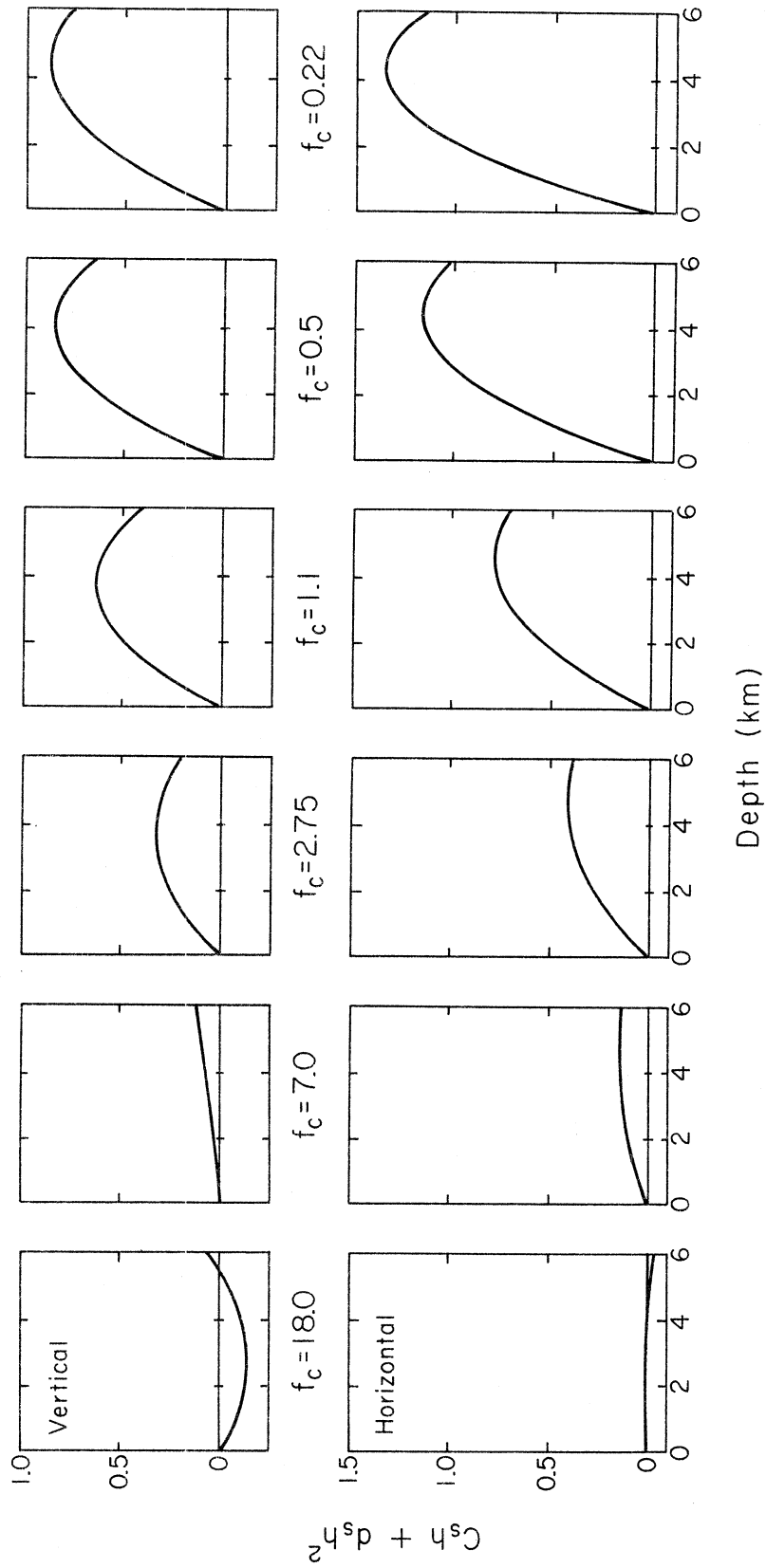
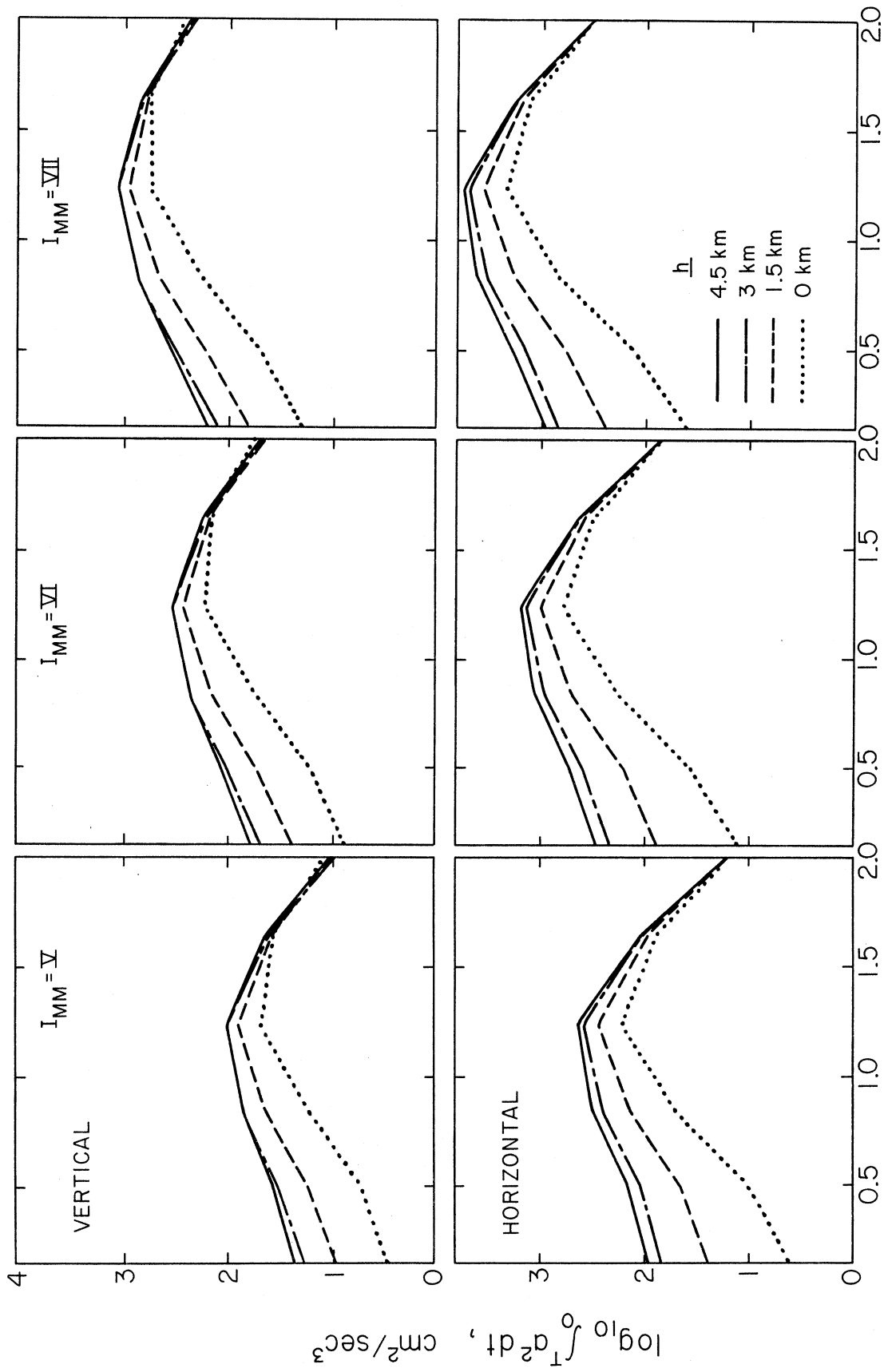


Figure 7
The values of $ch + dh^2$ versus depth

depth dependence in these two frequency bands is most probably small.

As Figure 7 shows, for the lowest frequency band, $f_c = 0.22$ Hz, and the horizontal component, the amplitude of $\int_0^T a^2(t)dt$ is roughly 20 times greater for $h = 4$ km than for $h = 0$ km. For the vertical component, it is approximately 8 times greater.

The values of $\log_{10} \int_0^T a^2(t)dt$, as calculated from equation (8) with the smoothed coefficients, are presented versus the center frequency in Figure 8. These curves show the trend for the depth to influence more the low frequency amplitudes of $\int_0^T a^2 dt$ for both components. The peak value of $\int_0^T a^2 dt$ is at $f_c = 2.75$ Hz for all depths except for the vertical component of $I_{MM} = VII$ where the maximum value of the integral is at $f_c = 7.0$ Hz.



$\log_{10} \omega_c$

Figure 8

The amplitudes of $\log_{10} \int_0^T a^2(t) dt$ computed from equation (8)

(with $\epsilon = 0$).

CORRELATIONS OF $\log_{10} \left[\int_0^T \left\{ \begin{matrix} a^2 \\ v^2 \\ d^2 \end{matrix} \right\} dt/\text{Duration} \right]$ WITH THE
MODIFIED MERCALLI INTENSITY AND THE DEPTH OF SEDIMENTS

Regression analyses are performed for the correlation of the frequency dependent average rates with the Modified Mercalli Intensity and the depth sediments in terms of the following model

$$\log_{10} \left[\int_0^T \left\{ \begin{matrix} a^2 \\ v^2 \\ d^2 \end{matrix} \right\} dt/\text{Duration} \right] \left\{ \begin{matrix} a \\ v \\ d \end{matrix} \right\} = a(\omega_c) + bI_{MM} + c(\omega_c)h + d(\omega_c)h^2 \quad (13)$$

The data and procedures used were identical to those outlined in the previous sections.

To group all of the data into a correlation for the average rate of growth of acceleration integrals, the approximations

$$\begin{aligned} \log_{10} \left[\int_0^T v^2 dt/\text{Duration} \right] &\approx \log_{10} \left[\int_0^T a^2 dt/\text{Duration} \right] - 2 \log_{10} \omega_c \\ \log_{10} \left[\int_0^T d^2 dt/\text{Duration} \right] &\approx \log_{10} \left[\int_0^T a^2 dt/\text{Duration} \right] - 4 \log_{10} \omega_c \end{aligned} \quad (14)$$

were employed in the analysis. Equations (14) follow directly from the approximations in equations (3) and (9).

The residuals, ϵ , as defined by

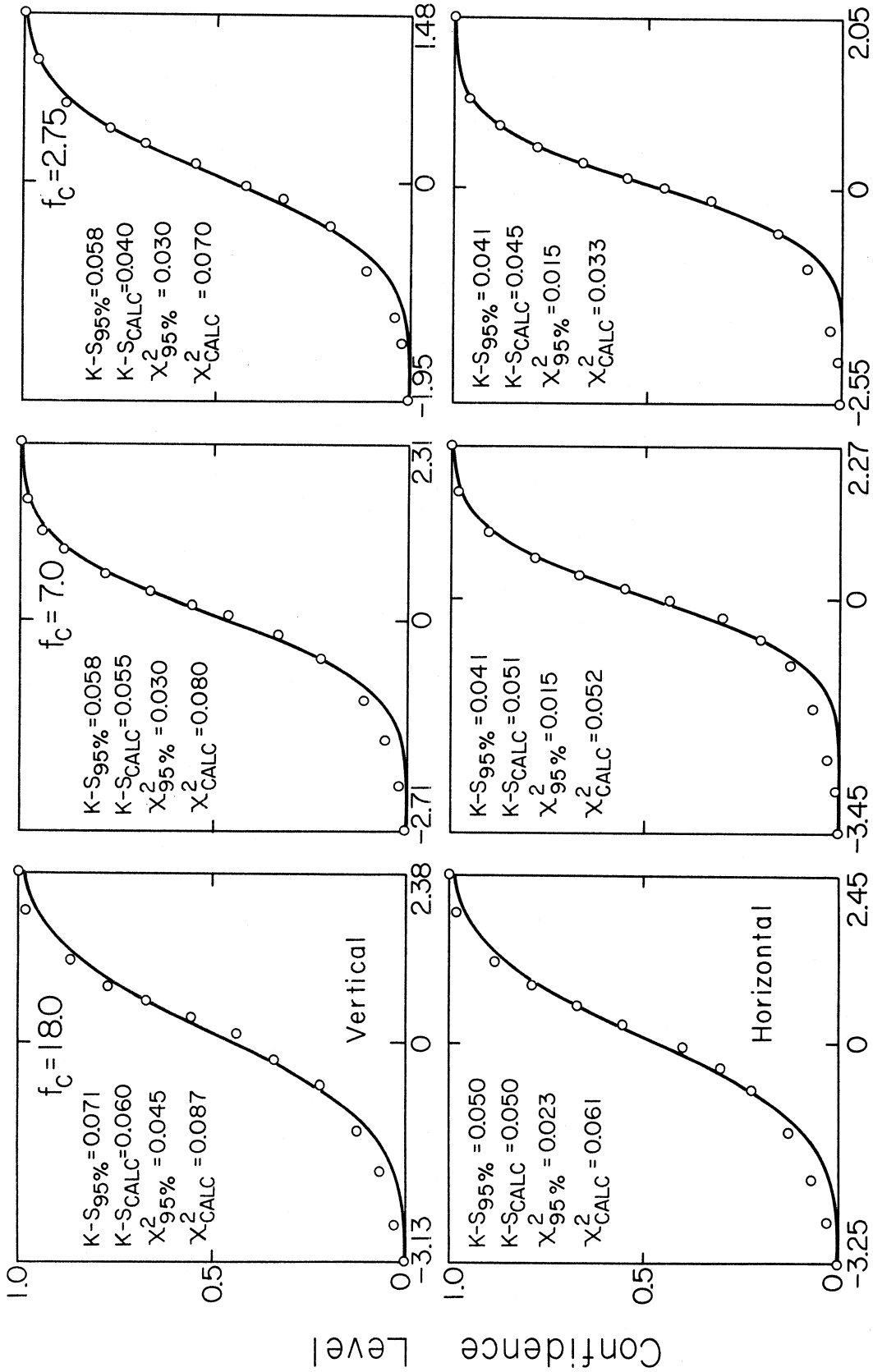
$$\epsilon = \log_{10} \left[\int_0^T a^2 dt/\text{Duration} \right] - \left\{ a + bI_{MM} + ch + dh^2 \right\}, \quad (15)$$

were analyzed in terms of their distribution functions which were chosen to represent the confidence level, p , that a particular ϵ will

not be exceeded. These distributions are shown in Figures 9a and 9b. As in the correlations with magnitude, a Gaussian distribution, equation (12), was fitted to the data (circles). This assumed distribution failed the Chi-Squared test at the 95% confidence level for all but two of the 12 residual functions. It passed the Kolmogorov-Smirnov test at the 95% confidence level for 8 of the functions. Considering the overall quality of fit, we chose to accept Gaussian approximation to $p(\epsilon)$.

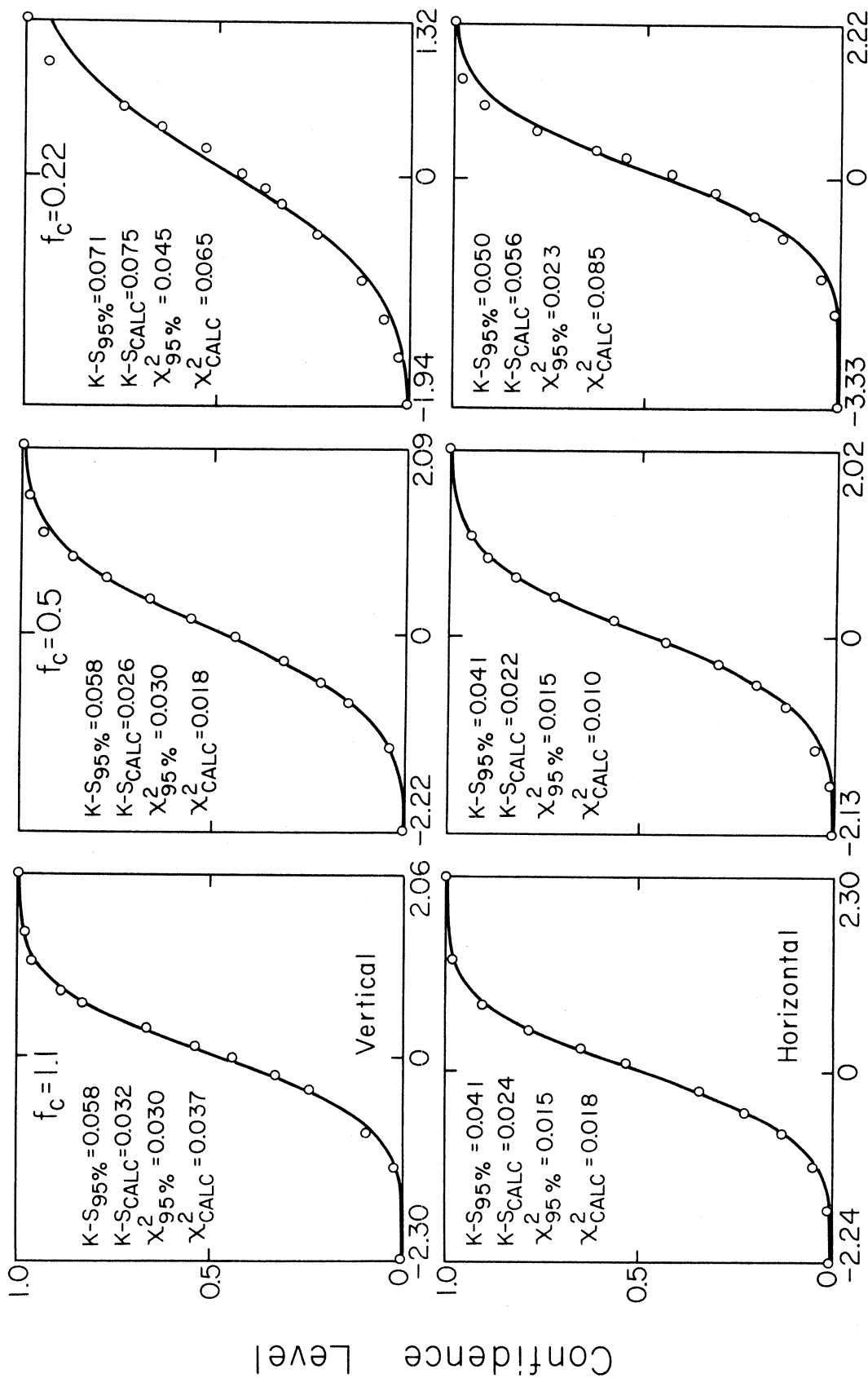
Table III lists the values of the coefficients a , b , c and d in equation (13) and the corresponding μ and σ in equation (12). These coefficients are plotted versus the center frequency in Figure 10. The dependence of the rates on the Modified Mercalli Intensity, shown by $b(\omega_c)$ in Figure 10, is similar to the dependence of the integrals, $\log_{10} \int_0^T a^2 dt$, on the intensity (Figure 5). As shown in this figure, the increase of the rates with intensity for the vertical component ranges from roughly 0.44 per I_{MM} (on the log scale) at $f_c = 0.22$ Hz to as much as 0.78 per I_{MM} at $f_c = 18.0$ Hz. The dependence of the rates on the depth of sediments for the correlations studied here is similar to those for the scaling in terms of magnitude (Westermo and Trifunac, 1978).

Figure 11 shows the values of $ch + dh^2$ in equation (13) plotted versus depth and calculated with the coefficients smoothed along ω_c . It can be seen that the depth dependence is greater at all frequency bands for the horizontal component. The average rate increases by roughly 18 times (on the linear scale) in comparing a depth of 4 km



$\epsilon (\omega_c)$
Figure 9a

The confidence level, p , versus the residual, ϵ , for the calculated residuals (circles) and for the fitted Gaussian distribution (solid curve). The Chi-Squared and Kolmogorov-Smirnov test results are listed for each distribution.



$\epsilon(\omega_c)$

Figure 9b

The confidence level, p , versus the residual, ϵ , for the calculated residuals (circles) and for the fitted Gaussian distribution (solid curve). The Chi-Squared and Kolmogorov-Smirnov test results are listed for each distribution.

TABLE III

Regression Coefficients in $\log_{10} \left[\int_0^T a^2(t) dt / \text{Duration} \right] = a + bI_{MM} + ch + dh^2$

VERTICAL COMPONENT

	$f_c = 18.0$	$f_c = 7.0$	$f_c = 2.75$	$f_c = 1.1$	$f_c = 0.5$	$f_c = 0.22$
a	-4.227	-2.591	-1.983	-3.052	-3.697	-3.255
Variance(a)	0.387	0.242	0.187	0.192	0.221	0.261
b	7.794	6.627	5.514	5.938	5.930	4.397
Variance(b) (x10)	0.618	0.386	0.299	0.306	0.353	0.416
c	-2.013	-0.620	0.908	2.810	4.103	3.417
Variance(c) (x10)	0.895	0.560	0.433	0.444	0.512	0.602
d	2.962	0.947	-1.990	-4.405	-5.495	-3.935
Variance(d) (x100)	1.608	1.006	0.778	0.797	0.919	1.082
μ (x100)	10.490	6.710	3.060	1.980	3.190	7.130
σ (x10)	10.436	7.408	5.687	6.157	7.627	7.779
h_{max}	3.398	3.273	2.283	3.189	3.734	4.341
No. of Data	372	558	558	558	558	372

HORIZONTAL COMPONENT

	$f_c = 18.0$	$f_c = 7.0$	$f_c = 2.75$	$f_c = 1.1$	$f_c = 0.5$	$f_c = 0.22$
a	-4.110	-2.152	-1.653	-2.755	-3.745	-3.650
Variance(a)	0.278	0.189	0.146	0.141	0.144	0.203
b	7.519	6.604	6.109	6.506	6.564	5.416
Variance(b) (x10)	0.443	0.302	0.233	0.224	0.230	0.323
c	-0.584	0.189	0.807	2.762	4.773	6.720
Variance(c) (x10)	0.642	0.438	0.339	0.326	0.333	0.469
d	0.106	-0.620	-1.134	-3.408	-5.312	-8.468
Variance(d) (x100)	1.153	0.786	0.609	0.585	0.599	0.843
μ (x100)	7.500	7.580	4.860	2.690	3.450	7.190
σ (x10)	10.361	7.783	5.815	6.195	6.517	8.106
h_{max}	27.605	1.521	3.556	4.052	4.492	3.968
No. of Data	744	1116	1116	1116	1116	744

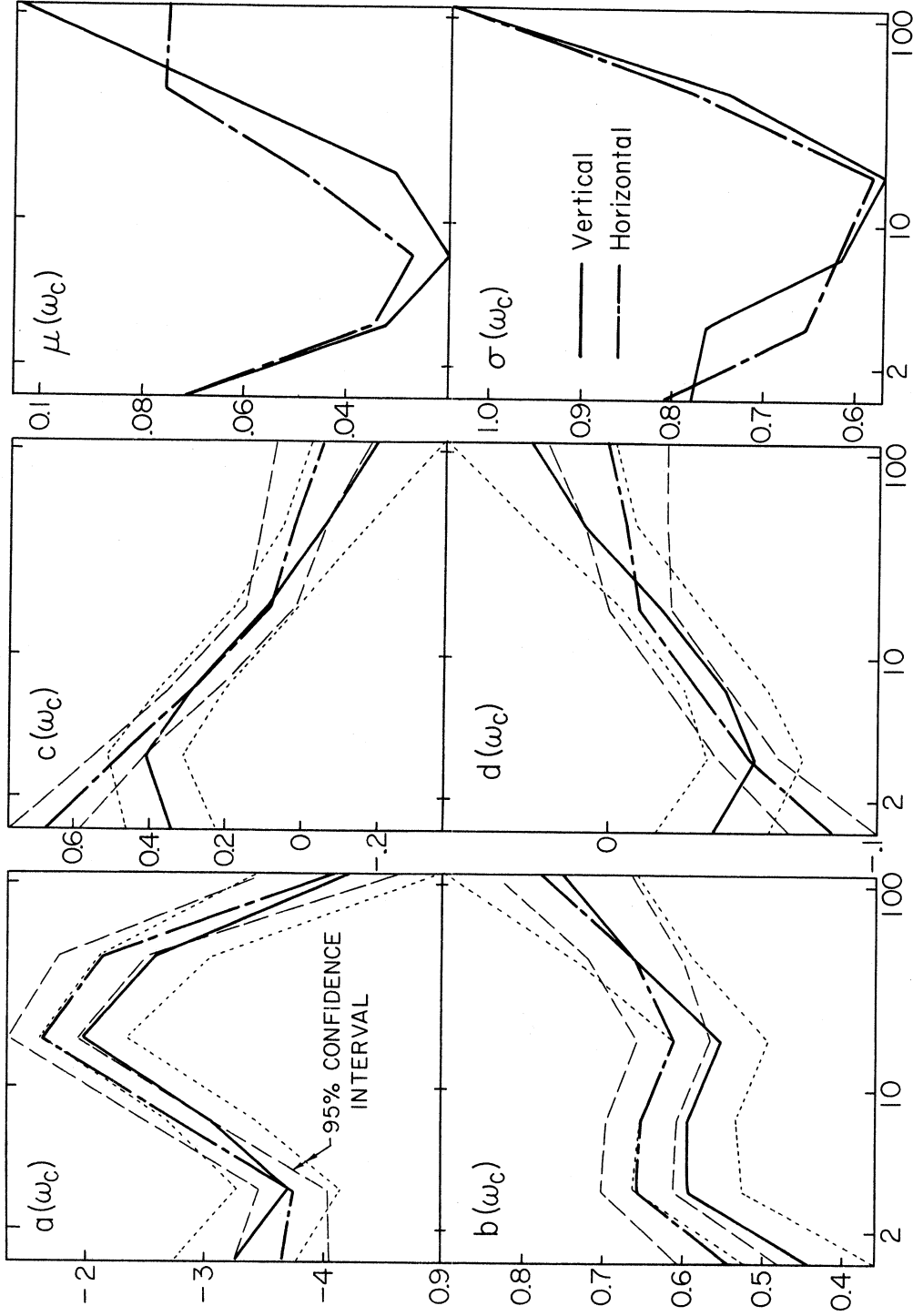
Center Frequency ω_c , rad/sec

Figure 10

The coefficients a , b , c , d , μ , and σ in equations (13) and (12) for horizontal and vertical acceleration, plotted versus $\omega_c = 2\pi f_c$ (for $f_c = 0.22, 0.5, 1.1, 2.75, 7.0$ and 18.0 Hz). The coefficients a , b , c , and d are bounded by the calculated 95% confidence intervals.

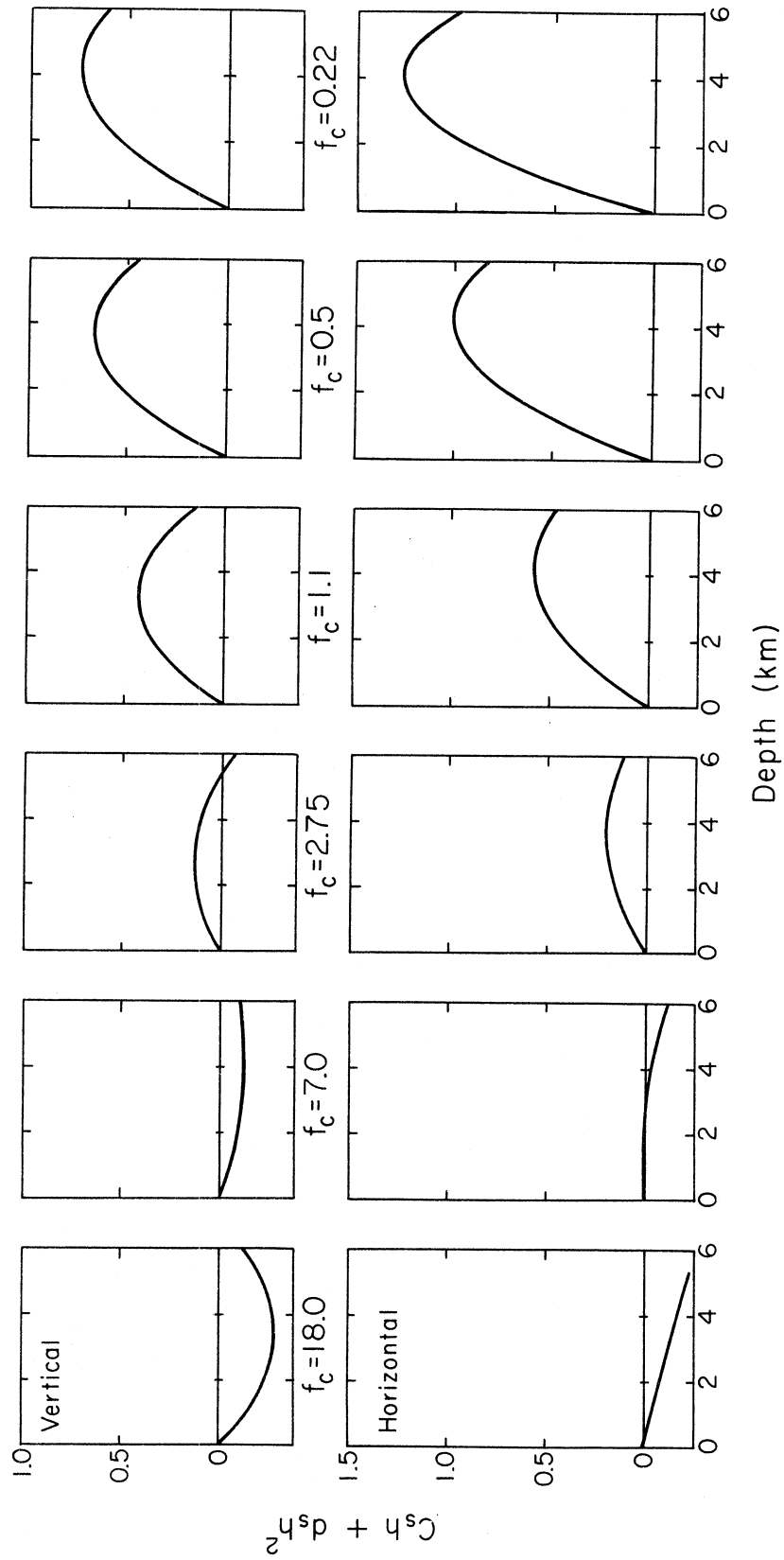


Figure 11

The amplitudes of $ch + dh^2$ versus depth.

to a zero depth for the low frequency band $f_c = 0.22$ Hz, for example. Only the four lowest frequency bands show a significant change (at a 95% confidence level) of rate with depth. For these frequency bands the peaks of $ch + dh^2$ are for h between 2.3 and 4.5 km (see h_{\max} in Table III).

The values of $\log_{10} \left[\int_0^T a^2 dt / \text{Duration} \right]$ calculated from equation (13) and using the smoothed coefficients are shown in Figure 12 for for the intensities $I_{MM} = V, VI, \text{ and } VII$ and for depths from zero to 4.5 km. This figure shows that for any intensity and for zero depths (hard rock sites) the average rate is smallest for the low frequencies, $f_c = 0.22$ Hz, and the largest at $f_c = 2.75$ Hz, with this difference, for example, being as much as 100 times the minimum (on the linear scale) for $I_{MM} = VII$.

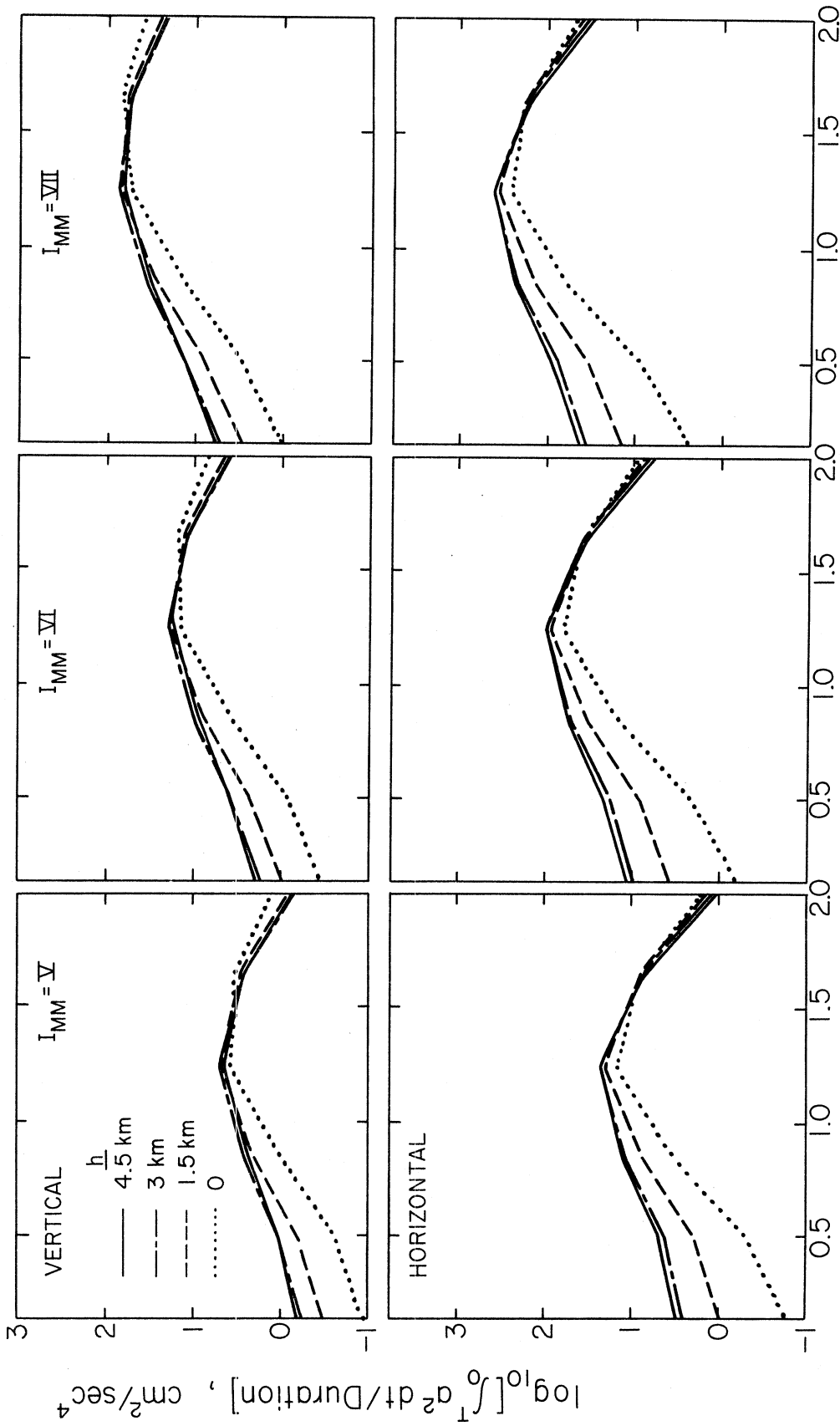


Figure 12

The amplitudes of $\log_{10} \left[\int_0^T a^2(t) dt / \text{Duration} \right]$ computed from equation (13) (with $\epsilon = 0$) for selected intensities and depths of sediments.

CONCLUSIONS

In this report we have examined the influence of the depth of sediments at the recording site on (i) the duration of strong motion, (ii) the integrals of the acceleration, velocity and displacement squared, and (iii) on the average rates of growth of these integrals during strong ground motion. Except for the depth dependent terms, the model equations used here are identical to those in Trifunac and Westermo (1976a,b).

For all three regression analyses, it was found that for the four lowest frequency bands, $f_c = 0.22, 0.5, 1.1$ and 2.75 Hz, the value of the duration, the integrals, and the average rates for the horizontal motions were consistently more dependent on the depth of sediments than the vertical motion.

The analysis of the duration shows that it is typically larger near the low frequency bands, $f_c = 0.22$ Hz, the difference in duration between the low frequency motions ($f_c = 0.22$ Hz), and high frequency motions ($f_c = 18.0$ Hz) being as much as 20 seconds. The variation in duration with frequency is larger for $I_{MM} = V$ compared to $I_{MM} = VI$ and VII. The duration increases roughly by 1.5 to 2.0 sec/km for the mid-frequency bands, ($f_c = 0.5, 1.1$ and 2.75 Hz). This increase is at a minimum of 0.8 sec/km for $f_c = 7.0$ Hz.

The amplitudes of the horizontal component of $\int_0^T a^2(t) dt$ at the lowest frequency band ($f_c = 0.22$ Hz) are roughly 25 times greater for $h = 4.5$ km than for a zero depth and are about 12 times greater

for the vertical component. The quadratic depth dependent term, $ch + dh^2$ in equation (8), reaches a maximum between the depths of 3 and 5 km for the four lowest frequency bands. The lack of data for depths beyond 6 km prevents us from concluding whether this is a local maximum or not. The growth of the integrals with depth is roughly 1.2 to 1.6 times larger (on the linear scale) for the horizontal component than for the vertical component. The analysis of the average rate of growth of these integrals shows a similar dependence on the depth of sediments.

ACKNOWLEDGEMENT

We thank John G. Anderson for critical reading of the manuscript and for useful suggestions.

This work was supported by a contract from the U.S. Nuclear Regulatory Commission.

Department of Civil Engineering
University of Southern California
Los Angeles, California 90007

REFERENCES

- Anderson, J.G., and M.D. Trifunac (1977). On uniform risk functionals which describe strong earthquake ground motion: definition, numerical estimation, and an application to the Fourier amplitude of acceleration, No. 77-02, Univ. of Southern California, Los Angeles.
- Arias, A. (1970). A measure of earthquake intensity, in Seismic Design of Nuclear Power Plants, Hansen (ed.), p. 438.
- Bolt, B.A. (1973). Duration of strong ground motion, Proc. Fifth World Conf. on Earthquake Engineering, Rome, 6-D, Paper No. 292.
- Cartwright, D.E., and M.S. Longuet-Higgins (1956). The statistical distribution of the maxima of a random function, Proc. Roy. Soc. London, Ser. A, 237, 212-232.
- Gutenberg, B., and C.F. Richter (1942). Earthquake magnitude, intensity, energy and acceleration, Bull. Seism. Soc. Amer., 32, 163-191.
- Gutenberg, B., and C.F. Richter (1956). Earthquake magnitude, intensity, energy and acceleration, Paper II, Bull. Seism. Soc. Amer., 46, 105-195.
- Hoel, P.G. (1971). Introduction to Mathematical Statistics, Fourth Edition, John Wiley and Sons, Inc., New York, 409 pp.
- Housner, G.W. (1952). Intensity of ground motion during strong earthquakes, Calif. Inst. of Tech., Pasadena.
- Meyer, S.L. (1975). Data Analysis for Scientists and Engineers, John Wiley and Sons, Inc., New York.
- Richter, C.F. (1958). Elementary Seismology, Freeman and Co., San Francisco.
- Thatcher, W., and T.C. Hanks (1973). Source parameters of southern California earthquakes, J. Geophys. Res., 78, 8547-8576.
- Trifunac, M.D., F.E. Udawadia, and A.G. Brady (1973). Analysis of errors in digitized strong-motion accelerograms, Bull. Seism. Soc. Amer., 63, 157-187.
- Trifunac, M.D., and V.W. Lee (1973). Routine computer processing of strong motion accelerograms, Earthquake Engr. Res. Lab., EERL Report No. 73-03, Calif. Inst. of Tech., Pasadena.
- Trifunac, M.D., and A.G. Brady (1975). A study on the duration of strong earthquake ground motion, Bull. Seism. Soc. Amer., 65, 581-626.

- Trifunac, M.D. (1976a). Preliminary analysis of the peaks of strong earthquake ground motion - dependence of peaks on earthquake magnitude, epicentral distance and recording site conditions, Bull. Seism. Soc. Amer., 65, 189-219.
- Trifunac, M.D. (1976b). Preliminary empirical model for scaling Fourier amplitude spectra of ground acceleration in terms of earthquake magnitude, source to station distance, and recording site conditions, Bull. Seism. Soc. Amer., 66, 1343-1373.
- Trifunac, M.D., and B.D. Westermo (1976a). Dependence of the duration of strong earthquake ground motion on magnitude, epicentral distance, geologic conditions at the recording site and frequency of motion, Dept. of Civil Engineering, Report No. 76-02, Univ. of Southern California, Los Angeles.
- Trifunac, M.D., and B.D. Westermo (1976b). Correlations of frequency dependent duration of strong earthquake ground motion with the Modified Mercalli Intensity and the geologic conditions at the recording stations, Dept. of Civil Engineering, Report No. 76-03, Univ. of Southern California, Los Angeles.
- Westermo, B.D., and M.D. Trifunac (1978). Correlations of the frequency dependent duration of strong earthquake ground motion with the magnitude, epicentral distance, and the depth of sediments at the recording site, Dept. of Civil Engineering, Report No. 78-12, Univ. of Southern California, Los Angeles.